Hindawi
Geofluids
Volume 2023, Article ID 1124656, 15 pages
https://doi.org/10.1155/2023/1124656

Research Article

Increasing Gas Production of Continuous Freeze-Thaw Hydrate Deposits Based on Local Reservoir Reconstruction

Pengfei Shen,[1,2] **Xiyu Mao**,[3] **Chaoqun Cui**,[2] **Xinwang Li**,[2] **Meng Li**,[2] **Li Chen**,[2] **and Dandan Liu**[4]

[1]*State Key Laboratory of Oil and Gas Reservoir Geology and Exploitation (Southwest Petroleum University), Chengdu 610500, China*
[2]*School of Mining and Geomatics Engineering, Hebei University of Engineering, Handan 056000, China*
[3]*Southwest Technology and Engineering Research Institute, Chongqing 400060, China*
[4]*School of Landscape and Ecological Engineering, Hebei University of Engineering, Handan 056000, China*

Correspondence should be addressed to Li Chen; chenli1981@hebeu.edu.cn and Dandan Liu; liudd12321@163.com

Received 10 October 2022; Revised 26 December 2022; Accepted 2 January 2023; Published 15 April 2023

Academic Editor: Zhenyuan Yin

The fracturing technology for increasing gas production based on hydrate reservoir reconstruction has been proven to have the application prospect of hydrate production. The main content of this work is to study the influence mechanism between multiple production wells after fracturing the reservoirs around horizontal wells. Simulation results indicated that the gas production rates and cumulative volume of released gas by using hydraulic fracturing were both higher than that by using the traditional depressurization method. The average gas-to-water ratio in this work has broken through the technical bottleneck of exploiting hydrate only by the traditional depressurization method. After the rock matrix around the horizontal well was fractured, the permeability of the reservoir in the fracturing area would be increased; thus, the propagation distance of pressure drop would be promoted. In addition, the penetration of the hydrate decomposition area between horizontal production wells was conducive to promoting the flow of decomposed gas and water to production wells. Besides, the hydraulic fracturing method to increase the permeability of the reservoir around the production well is very effective for the gas production of low-permeability natural hydrate deposits. The best distance between production wells was recommended to be 45~60 m, and it was recommended to provide appropriate heat in the area between the two wells to accelerate the decomposition of hydrate.

1. Introduction

Natural gas hydrates (NGHs) are considered one of the most promising energy sources in the future due to their huge potential reserves, strong gas concentration capacity, high energy density, wide resource distribution, and other characteristics [1–3]. As a strategic reserve resource, mastering more advanced development technology of complex geological oil and gas resources can better resist external risks and improve national energy security. At present, NGH deposits mainly include marine hydrate deposits and permafrost hydrate deposits. The principle of recovering natural gas from NGH deposits in two different environments is to destroy the stable occurrence state of hydrate reservoirs [4, 5]. For example, when the stability of hydrate is damaged due to the pressure drop or temperature rise in the sediments, the hydrate will be decomposed into methane gas and water. There are four prevalent techniques to recover gas from hydrate deposits, such as depressurization [6, 7], thermal stimulation [8, 9], inhibitor injection [10], and CO_2/N_2 replacement [11, 12]. In general, the depressurization method, in which the gas recovery from hydrate

deposits by lowering the pressure below that of the hydrate stability, is considered to be the most economic and simple method.

NGH is a highly complex resource with dual properties of solid and fluid. The development process of hydrate is a multiphase, multicomponent, and nonisothermal physical and chemical seepage process. This process involves the transition of NGH from solid to gas and liquid in the reservoir, the flow of gas-liquid mixture in the reservoir medium, the change of reservoir permeability, the change of pore pressure, gas expansion, etc. [13, 14]. At present, there is a huge investment in the pilot production of offshore NGH, and the gap between the level of natural gas output and commercial exploitation is obvious [15, 16]. The adoption of high-frequency pilot production will shorten the gap between actual exploitation and commercial exploitation, but it will undoubtedly increase the global economic burden. In order to realize the development of NGH resources in permafrost regions and lay a good foundation for large-scale marine development of NGH, many countries are gradually carrying out research and test on long-term mining methods of NGH in permafrost regions. However, in addition to mining methods, NGH development in permafrost regions still faces two problems. One is that the destruction of NGH deposits may lead to the escape of natural gas. The second is that the continuous freezing and thawing process of the NGH reservoir results in the increase of pore pressure and the decrease of structural strength, causing geological disasters such as thawing settlement, rheology, and fracturing of the reservoir [17]. However, the key problem of hydrate development in permafrost regions is still the fact that the permeability of natural gas hydrate reservoirs in permafrost is extremely low, which leads to low gas production efficiency of natural gas hydrate development. Therefore, the development of hydrate resources in permafrost regions still needs to solve the problem of low permeability of reservoirs.

The field trial mining of NGH in permafrost regions is conducive to the implementation of commercial mining. At present, many countries have begun to carry out research on the development technology of NGH resources in permafrost regions. The Messoyakha NGH deposit is proved to contain a large amount of NGH, and the depressurization test production was carried out in 1969. During this period, the free water generated by NGH decomposition was converted into ice at low temperatures, resulting in the total gas production being several orders of magnitude lower than the expected gas production from hydrate decomposition, which shows that the emergence of ice will hinder the NGH production efficiency in permafrost regions [18]. In 2002, the United States, Canada, Japan, Germany, and India jointly conducted large-scale pilot mining in the frozen soil area of the Mackenzie Delta in the Arctic cold environment. The production test results show that the generation of ice causes the low-permeability area near the production well and the formation of blockage, leading to a significant reduction in the gas production rate [19]. In 2003, the US Department of Energy and the US Geological Survey determined the research plan for NGH pilot production in the frozen soil area on the northern slope of Alaska. So far, two short-term mining tests have been carried out in this area. During the application of the carbon dioxide replacement method, the replacement rate is low due to the low temperature of free water in the reservoir transforming into ice. This indicates that the reservoir occurrence geology in this area has changed during the hydrate development process. If the reservoir deformation and damage are serious during the hydrate development process, corresponding control measures in the mining area are required to avoid this situation [20]. The above pilot production test shows that the generation of ice during NGH decomposition in frozen soil area greatly reduces the permeability of the reservoir and significantly enhances the anisotropy and difficulty of fluid flow in the reservoir.

NGH in the permafrost region of the Qinghai Tibet Plateau in China has a high occurrence complexity, and the soil medium is extremely sensitive to temperature [21]. Under the global warming environment, NGH is undergoing strong degradation [22]. The degradation of frozen soil will inevitably result in the decomposition, release, migration, and redistribution of critical NGH [23]. Even if NGH in the permafrost region of the Qinghai Tibet Plateau has no value for industrial exploitation, the decomposition of NGH in the critical state will pose a great threat to global warming and the international environment [24]. The research on the interaction between NGH and reservoir fracture medium and the prevention and control of potential risks of gas leakage in the permafrost region of the Qinghai Tibet Plateau in China is relatively backward, so it is urgent to carry out in-depth research. For NGH research in permafrost regions of the Qinghai Tibet Plateau, the first is to evaluate the geological stability of the reservoir during NGH decomposition, and the second is to clarify the interaction between NGH and reservoir pores [24]. Therefore, even if some hydrate resources in permafrost regions in China have no commercial exploitation value, it is important to effectively control the fossil energy contained in these hydrate resources before they cause major environmental disasters and hazards. In addition, the development of hydrate resources in permafrost regions in China is imperative, and if hydrate resources can be effectively developed at a low development cost, it will bring huge environmental benefits with minimal economic losses. Therefore, the focus of this research work is to find the simplest and most economical way to reconstruct the hydrate reservoir. It is expected that this local reconstruction method can ensure the decomposition of hydrate as much as possible in the mining area of the frozen soil area.

From 2008 to 2009, China's "Natural Gas Hydrate Scientific Drilling Project in Qilian Permafrost Area" was implemented in Muli District, Qilian Permafrost Area, and NGH physical samples were successfully drilled for the first time in the DK-1, DK-2, and DK-3 [25–27]. In 2013, China successfully drilled NGH physical samples with a single layer thickness of more than 20 m in the DK-9 scientific drilling test well again [28]. In 2020, Lu et al. found the coexistence system of NGH, oil, and natural gas for the first time in this area [29]. Considering that the permafrost area of the

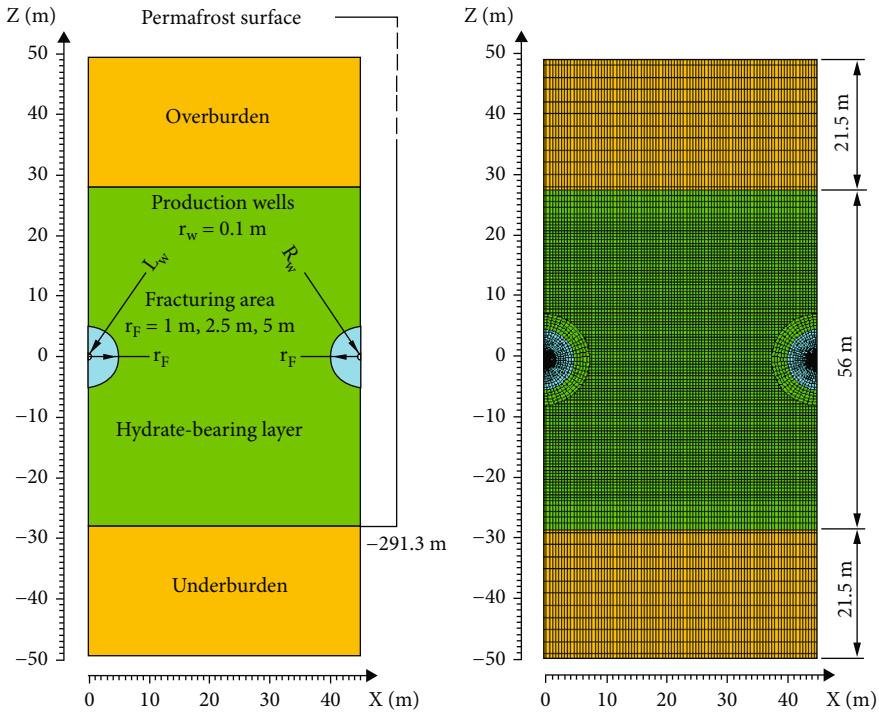

Figure 1: Layout and domain discretization of two-point horizontal well system.

Qinghai Tibet Plateau is about 1.5×10^6 km^2, NGH reserves in permafrost regions of the Qinghai Tibet Plateau have high expectations and development potential prospects. However, China's investment in research on NGH mining technology in permafrost regions of the Qinghai Tibet Plateau and research on prevention and control measures for reservoir gas leakage risk is weak [30]. For NGH resources in the permafrost region of the Qinghai Tibet Plateau with very low intrinsic permeability, the current research shows that even if the thermal injection method is used to extract the NGH resources, the gas production effect is very poor. Therefore, the most practical method for NGH sediment mining in low-permeability permafrost regions is to increase the permeability of sediments [31]. In previous work, the new combination of fracturing technology and depressurization method was applied to increase the permeability around the production well; the simulation results showed that the increase of the permeability can increase the gas production to 2.1 times with increasing the radius of the fracture zone from 0 to 4 m for 30 years [32]. At present, the research on reservoir reconstruction in permafrost regions is also increasing and becoming a hot spot.

In addition, reservoir characteristics play an important role in controlling the decomposition and redistribution of NGH in the Qilian permafrost region. Based on NGH borehole data in the permafrost region of the Qinghai Tibet Plateau, it was found that the ore deposits are mainly fracture type, followed by fracture pore mixed type, and the proportion of pure pore occurrence is very low [33]. NGH occurs in the fracture surface and pores of mudstone, fine sandstone, siltstone, oil shale, and fine to medium sandstone in the form of thin layer, sheet, and block. The hydrate saturation varies greatly and is unevenly distributed. Zhu et al. found that Qilian Mountain NGH has the characteristics of thin permafrost zone, shallow burial depth, complex gas composition, and genesis through drilling NGH cores [34]. The NGH-bearing core gives off bubbles and water drops after decomposition, leaving honeycomb structure characteristics. Qu et al. collected the mudstone core of a fractured NGH reservoir in the permafrost region of Qilian Mountains and conducted physical rock experiments such as acoustic wave, porosity, and permeability of the sample [35]. It is found that there are coin-shaped fractures and infinite-length fractures in the fractured NGH reservoir in the permafrost region of Qilian Mountains, of which the infinite-length fracture is the main form. Li et al. conducted numerical analysis and laboratory experiments on NGH samples in the permafrost region of Qilian Mountains and found that the formation and accumulation of NGH were controlled by the subsidence and uplift of permafrost structures, while the migration and accumulation of natural gas were controlled by faults and tight strata [36]. Lin et al. described the thickness of the permafrost layer and the logging response of the NGH reservoir in combination with conventional logging and imaging logging parameters and found that NGH in the Qilian frozen soil area generally occurs in the fractures and pore spaces of host rocks with layered or microdisseminated structures, and the occurrence mainly follows the suspension mode [37]. This shows that the occurrence conditions of hydrate reservoirs in the permafrost region of the Qinghai Tibet Plateau in China are complex, and even if there are many ways to transform the reservoirs, they cannot be applied to the large-scale hydrate development environment. Therefore, for the development

of hydrate in permafrost areas, when selecting the method to increase the permeability of the hydrate reservoir, it is necessary to comprehensively consider the occurrence characteristics of the hydrate reservoir and try to obtain better gas production effect under the condition of small area reservoir reconstruction.

The clarification of fracture morphology and NGH occurrence mode in the Qilian permafrost region can improve the understanding of reservoir properties and NGH accumulation control, which is crucial for evaluating the resource potential of gas hydrate accumulation in the Qilian permafrost region [38]. Wang et al. comprehensively analyzed all aspects of reservoir fracturing, including brittleness, fracture toughness, and fracturing index model, to provide an overall view of offshore NGH reservoir fracture generation. In this study, the main reservoir stimulation methods are summarized into four aspects: hydraulic fracturing, jet fracturing, overburden modification, and fracturing grouting. Through comparison, it is found that split grouting is the most promising method to achieve the two objectives of reinforcement of the reservoir skeleton and seepage enhancement. At the same time, the study also points out that further development is needed to obtain reliable NGH reservoir fracturing results and bridge the gap between conceptual design and practical application of reservoir stimulation. This shows that there is still a big gap between the current methods of improving gas hydrate production based on reservoir reconstruction and actual production testing [39]. Since the initial purpose of this paper is to study the effect of hydrate exploitation after fracturing in the reservoir around the exploitation well, this paper believes that the fracturing technology is more consistent with the characteristics of horizontal wells in the hydrate reservoir in the frozen soil area. Therefore, hydraulic fracturing technology is preferred for the fracturing method of this work.

Therefore, the combination of depressurization and hydraulic fracturing is considered to be an effective and practical method. In addition, the fractured rock produced by hydraulic fracturing will not flow along the production well, so there is no need to worry about the displacement of the production well. The research focus of this paper is to find a relatively high gas production method under the condition of relatively simple reservoir reconstruction. In this work, the feasibility of the reservoir around the horizontal well in the rock after hydraulic fracturing is analyzed, and on the basis of the reservoir local reconstruction by fracturing technology, the sensitivity analysis of the impact of different permeability in the reservoir fracturing area on the gas production by hydrate exploitation is carried out.

Hence, in this work, in order to promote the development of hydrate reservoir mining technology in the permafrost region, the thickest hydrate layer at DK-2 station in the Qilian Mountains permafrost region is used as the hydrate sedimentary zone for simulation. Hydraulic fracturing technology is used to fracture the rock around the horizontal production well to form a fracturing area with high permeability around the production well, so as to provide a smooth flow path for pressure transmission. Finally, the production behavior after adopting this method and the sensitivity of gas production behavior to the fracturing area and the permeability in the fracturing area are evaluated. The simulation results show that the relatively high permeability area produced by fracturing technology outside the horizontal exploitation well plays an important role in the exploitation of frozen soil areas.

2. Production Method and System Description

2.1. Layout and Domain Discretization of Two-Point Horizontal Well System. From 2008 to 2009, Zhen-Quan et al. carried out a scientific pilot drilling project for natural gas hydrate near Muli area, a permafrost region in the Qilian Mountains, with borehole numbers of DK-1, DK-2, DK-3, and DK-4 [40]. The white ice-like physical sample was directly drilled, and the burning phenomenon was observed. It was detected as natural gas hydrate by a laser Raman spectrometer, which was the first natural gas hydrate discovered in China's land area. The natural gas hydrate is often exposed in the fractures and pores of the rock stratum, which is obviously controlled by the fractures. Its vertical distribution is discontinuous, and it mainly occurs between 130 and 400 m underground. Taking the DK-2 drilling project as an example, the borehole has proved that there are four hydrate layers with depths of 144.4-152.0 m, 156.3-156.6 m, 235.0-291.3 m, and 377.3-387.5 m. Among them, the hydrate layer with a buried depth of 235.0-291.3 m is the most recoverable. Therefore, this work is based on the geological background of the hydrate in this layer to carry out mining simulation research.

As shown in Figure 1(a), the third hydrate-bearing layer (HBL) of DK-2 with a thickness of 56 m is selected for simulation, and the buried depth of HBL bottom is 291.3 m. In addition, the thickness of the overburden layer (OB) and underburden layer (UB) on both sides of the HBL is 21.5 m, which can ensure the fluid exchange and heat transfer between the HBL, OB, and UB during the production process. The longitudinal dimension of the simulation area in this work is 99 m. In view of the difficulty and low efficiency of hydrate mining in permafrost regions, according to the existing literature on hydrate mining by numerical simulation, the maximum range of a single horizontal well mining period in 30 years is about 15~20 m [32]. This research work should not only consider the impact between dual horizontal wells but also consider the increase in gas production of horizontal wells after the use of fracturing technology. Therefore, the spacing between two horizontal wells is 45 m; that is, the transverse distance of the entire simulation area is 45 m.

In addition, the left well (L_W) and right well (R_W) are located in the middle of the simulation area, and half of L_W and R_W are selected to form the smallest repeatable unit. The length of L_W and R_W are assumed to be 1000 m. The fracturing area with the radius of r_F is around L_W and R_W, and the radius of r_F is a variable. In this study, the horizontal well is expected to be used as the fracturing well, and the reservoir around the horizontal well is partially damaged by hydraulic fracturing, so the fracturing area is generally near

Table 1: Model parameters and initial conditions of HBL at site DK-2.

Parameter	Value
Thickness of OB, HBL, and UB	21.5, 56, and 21.5 m
Distance between L_W and R_W	45.0 m
Bottom position of HBL	-291.3 m
P_B and T_B	4.19 MPa and 277.84 K
Initial saturation in HBL	$S_H = 0.40$, $S_A = 0.60$
Gas composition	100% CH_4
G_1 and G_2	0.013 K/m and 0.028 K/m
k_0 of HBL, OB, and UB	1×10^{-15} m^2
Porosity ϕ (all formations)	0.30
$k_{\Theta RW}$ and $k_{\Theta RD}$	3.1 and 1.0 W/m/K
Composite thermal conductivity model [8]	$k_{\Theta C} = k_{\Theta RD} + \left(S_A^{1/2} + S_H^{1/2}\right)(k_{\Theta RW} - k_{\Theta RD}) + \phi S_I k_{\Theta I}$
Capillary pressure model [8]	$P_{cap} = -P_{01}\left[(S^*)^{-1/\lambda} - 1\right]$ $S^* = (S_A - S_{irA})/(S_{mxA} - S_{irA})$
S_{irA}&S_{irG}	0.30 & 0.05
λ & P_{01}	0.45 & 10^5 Pa
Relative permeability model [8]	$k_{rA} = (S_A^*)^n$ $k_{rG} = (S_G^*)^{nG}$ $S_A^* = (S_A - S_{irA})/(1 - S_{irA})$ $S_G^* = (S_G - S_{irG})/(1 - S_{irA})$
n & n_G	3.572

the production well. Therefore, we use radius r_F to describe a range of fracturing areas around the production well. The permeability of the reservoir in this fracturing area is considered to be improved, and it is assumed that the permeability of the fracturing reservoir is consistent. The grid division of the whole simulation area is shown in Figure 1(b), and the hybrid grid consisted of 12588 elements. A cylindrical fine grid of 7.5 m is divided outside L_W and R_W, which can ensure the accuracy of calculation. Except for the cylindrical fine mesh, the distance interval of the horizontal mesh is uniformly 0.5 m. However, in the longitudinal direction, the longitudinal interval in HBL is 1 m, and the longitudinal interval in OB and UB is 2 m. The grid along the production well direction is selected with a length of 1 m for gas production calculation.

2.2. Model Parameters and Initial Conditions. The production behavior of the HBL at DK-2 is calculated by the parallel version of TOUGH+HYDRATE (T+H) code. Table 1 shows the initial conditions of HBL at the DK-2 station. The radius of L_W and R_W is $r_W = 0.1$ m, and L_W and R_W are geometrically symmetrical in the simulation area. The porosity of L_W and R_W is set to 1.0, the absolute permeability (k_0) inside L_W and R_W is set to 5000 Darcies, and the capillary pressure of L_W and R_W is set to 0. The initial hydrate saturation (S_H) and aqueous saturation (S_A) of HBL are 0.4 and 0.6, respectively. The initial S_A of OB, UB, and fracturing area is 1.0. The porosity of all formations is 0.3, and k_0 of OB, UB, and HBL is 1 mD. It is worth mentioning that k_0 in the fracturing area is a variable parameter, which is related to the technical level of actual construction. The gas composition in the HBL area is 100% methane. The models of composite thermal conductivity and capillary pressure selected are shown in Table 1, and the wet thermal conductivity $K_{\Theta RW}$ and the dry thermal conductivity $K_{\Theta RD}$ are 3.1 W/m/K and 1.0 W/m/K, respectively. The attenuation model index n and gas permeability reduction exponent n_G in the relative permeability model is 3.572, and the irreducible aqueous phase saturation S_{irA} and irreducible gas saturation S_{irG} are 0.30 and 0.05, respectively. In addition, the initial temperature T_B at the bottom of the HBL is 277.84 K, and T_B is calculated according to the thermal gradient within (G_1) and under (G_2) the frozen layer. G_1 and G_2 are 0.013 K/m and 0.028 K/m, respectively. The initial pressure P_B at the bottom of the HBL is 4.19 MPa, and P_B is calculated according to the rock density of the permafrost deposits, the thickness of the permafrost layer underground, and the fluid density under the permafrost layer.

2.3. Production Method and Strategy. The main content of this work is to study the influence mechanism between multiple production wells after fracturing the reservoirs around horizontal wells. Therefore, the depressurization production method is adopted to compare the gas production improvement effect of production wells after local reservoir reconstruction. The fracturing area formed by the crushing of the circumferential rock of L_W and R_W can be realized by hydraulic fracturing technology. The formation of the

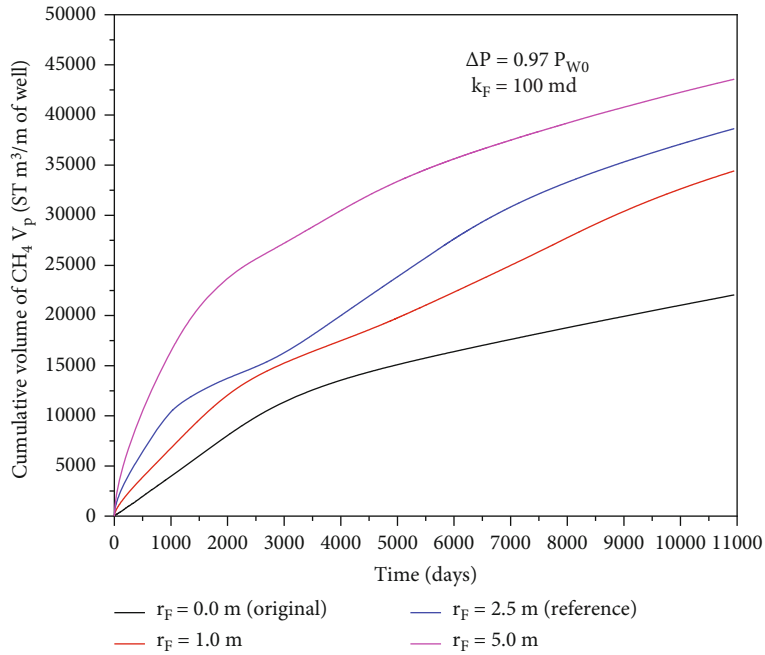

FIGURE 2: V_P from the production wells with different r_F.

fracturing area around L_W and R_W is essential to improve the flow capacity of gas and liquid in the rock around the production well during the hydrate production process. Hence, the sensitivity analysis of intrinsic permeability in fracturing area (k_F) to gas production needs to be considered, and the permeability values $k_F = 1$, 2, 10, 100, and 1000 mD are used in this study, respectively. In addition, the scope of the fracturing area will have an important impact on the gas production behavior of the entire hydrate layer. $r_F = 0$, 1.0, 2.5, and 5.0 m is employed to simulate the fracturing area in the reservoir rocks surrounding L_W and R_W, and the only difference from the HBL is that the fracturing area has higher intrinsic permeability. Therefore, this work combines the advantages of the hydraulic fracturing method and the depressurization method and applies the hydraulic fracturing method to a two-point horizontal well system to continuously decompose and exploit natural gas from permafrost hydrate deposits.

3. Simulation Results

3.1. Evaluation of the Productions with Different r_F

3.1.1. Gas and Water Production with Different r_F. In this work, all cases are calculated for 30 years. The case of $r_F = 0$ m, $k_F = 1$ mD is the original case. Even though the simulation result shows that the gas production effect is better when $r_F = 5$ m, $k_F = 1000$ mD. Considering that it is more practical and the case of $r_F = 2.5$ m, $k_F = 100$ mD is set to be the reference case. The reference case is set to compare with the production behavior of the original case, thus reflecting the advantages of this research work. This work does not use the best effect as the reference case, because the case of $r_F = 2.5$ m and $k_F = 100$ mD is more in line with the current construction technology. This is also the ultimate goal of this work, that is, to obtain more cost-effective gas production under the minimum and optimal economic conditions, so as to provide more appropriate guidance for the local reconstruction of hydrate reservoirs in the future. In order to obtain greater gas production, the driving force for depressurization (ΔP) is 0.97 P_{W0}.

Figure 2 shows the cumulative volume of the produced methane gas (V_P) from L_W and R_W with $r_F = 0$ m, 1.0 m, 2.5 m, and 5.0 m, respectively. As shown in Figure 2, V_P in the original case (without fracturing technology) is almost 2.2×10^4 m^3 per meter along the production well under standard state (ST) at the end of the 30-year production period. In the reference case ($r_F = 2.5$ m), the total cumulative methane gas is more than 3.8×10^4 ST m^3, which is a big improvement compared to the original case. The increase in V_P indicates that the fracturing area caused by the hydraulic fracturing method promotes the propagation velocity of pressure. Besides, it is found that more than 60% of gas production is produced in the first 10 years in the reference case. This phenomenon indicates that the methane gas flow rate slows down in low-permeability deposits at the later stage of the gas decomposition process. Comparing the four cases, it is shown that the wider the r_F is, the larger the V_P would be produced, and it indicates the obvious effect of the hydraulic fracturing method on the gas release from the hydrate deposits.

However, the increase rate of V_P slows down gradually regardless of whether fracturing technology is used. This is mainly due to the fact that gas and water generated by the decomposition of hydrate far from the production well are not easy to flow to the production well in the later stage of

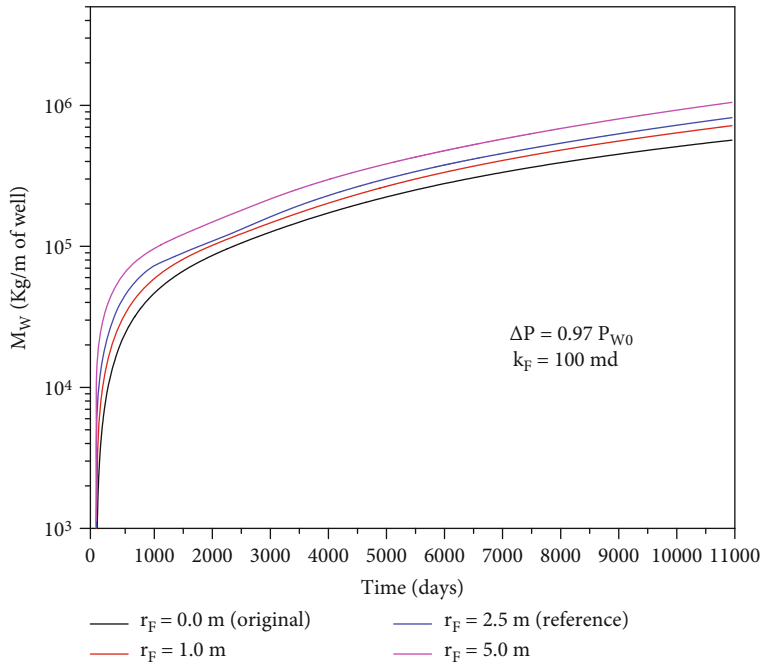

Figure 3: M_W from the production wells with different r_F.

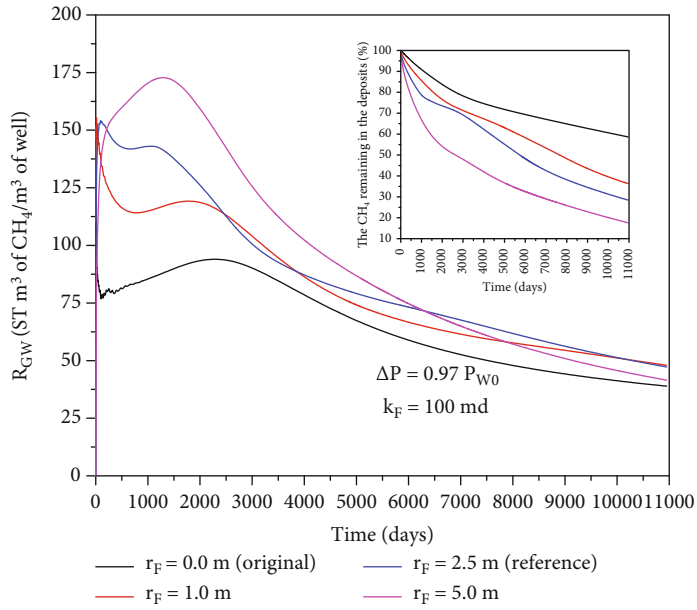

Figure 4: R_{GW} and R_H with different r_F.

production. Another discovery is that even if $r_F = 1.0$ m, the gas production of low-permeability reservoirs has significantly increased. This is mainly because after the rocks around the production well are fractured, the depressurization pressure will be effectively transmitted to the reservoir outside the production well, and the natural gas and water generated from the decomposition of hydrate will flow more easily to the production well, thus increasing the multiphase fluid flow flux of the production well. Therefore, increasing flow flux from the low-permeability reservoir to the production well will have more practical significance for the actual exploitation of the low-permeability reservoir.

Figure 3 shows the cumulative mass of water (M_W) from L_W and R_W with $r_F = 0$ m, 1.0 m, 2.5 m, and 5.0 m, respectively. As shown in Figure 3, with the increase of r_F, M_W will gradually increase. The final M_W in the original case and reference case are 5.67×10^5 kg and 8.18×10^5 kg, respectively. By comparing the reference case and the original case, it is

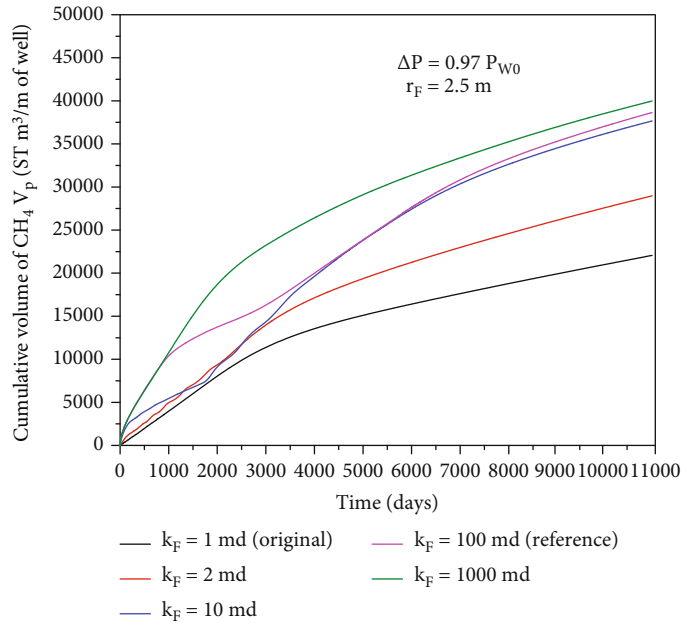

Figure 5: V_P from the production wells with different k_F.

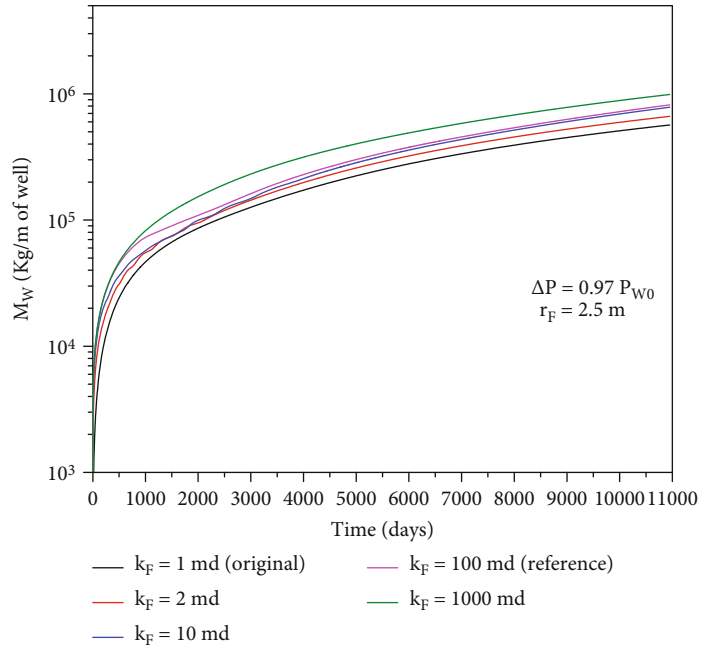

Figure 6: M_W from the production wells with different k_F.

found that the growth multiple of gas production is higher than that of water production, which indicates that fracturing technology is more conducive to the production of hydrate decomposition gas after fracturing the reservoirs around the production well, which is a key improvement of gas production in low-permeability reservoirs. Another reason why the water generated by hydrate decomposition flows relatively less to the production well may be that some free water forms solid ice particles due to the existence of low temperatures during hydrate exploitation.

3.1.2. Gas-to-Water Ratio and the Remaining Hydrate Deposits with Different r_F. Figure 4 shows the gas-to-water ratio R_{GW} ($R_{GW} = 1000V_P/M_W$) and the remainder of hydrate deposits R_H with $r_F = 0$ m, 1.0 m, 2.5 m, and 5.0 m, respectively. R_{GW} are a critical parameter for hydrate exploitation. The water phase was the dominant factor for hydrate dissociation, while the gas phase flow had a negative effect. The ratio curves rise sharply in the first year and then decrease to a lower level gradually. R_{GW} of the original case is less than the cases using the hydraulic fracturing method.

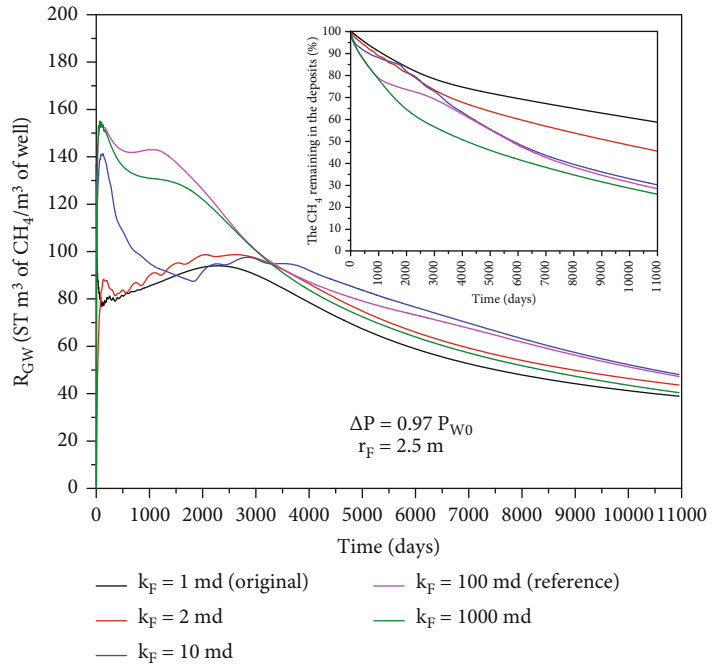

Figure 7: R_{GW} and R_H with different k_F.

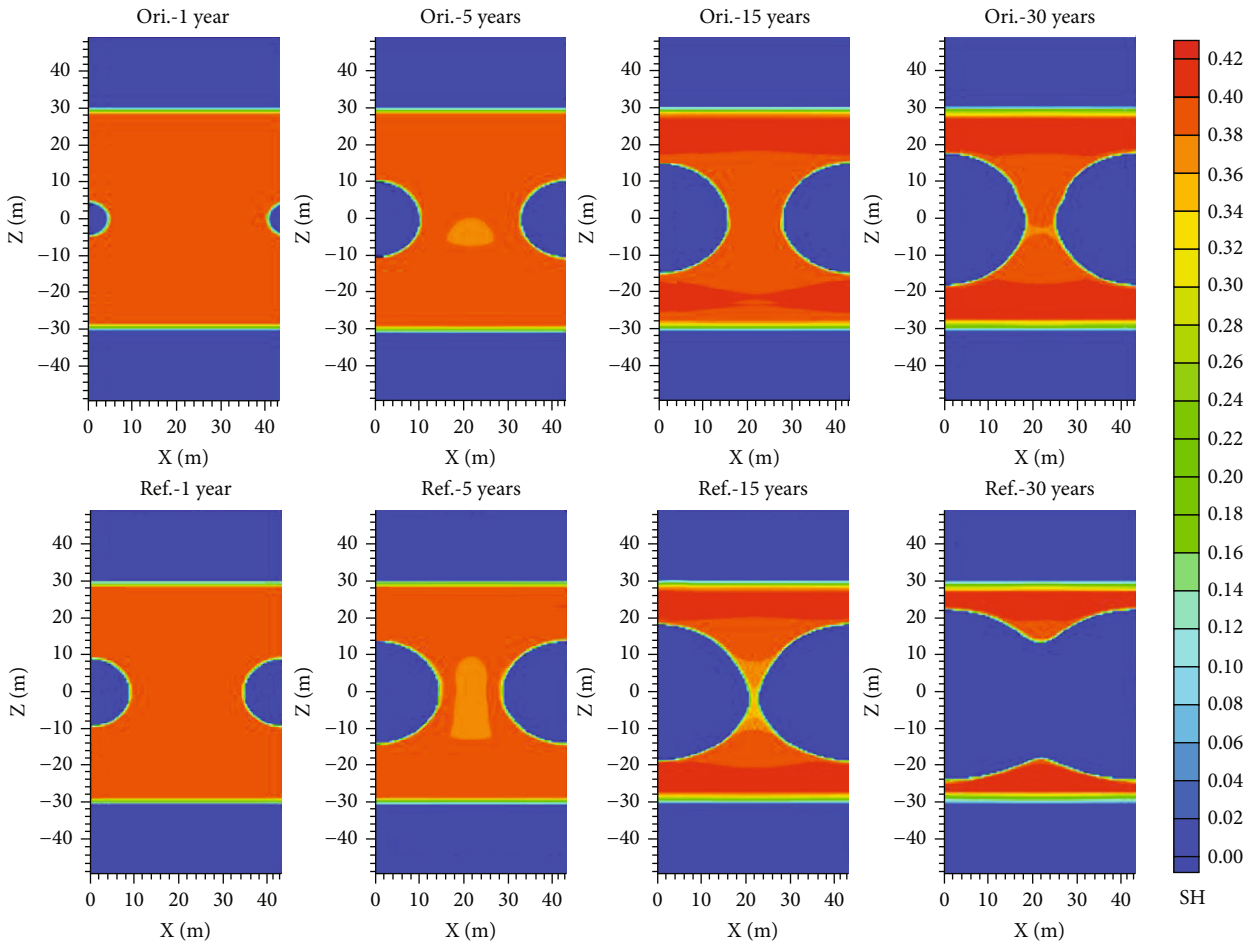

Figure 8: The spatial distributions of S_H in the original and reference cases.

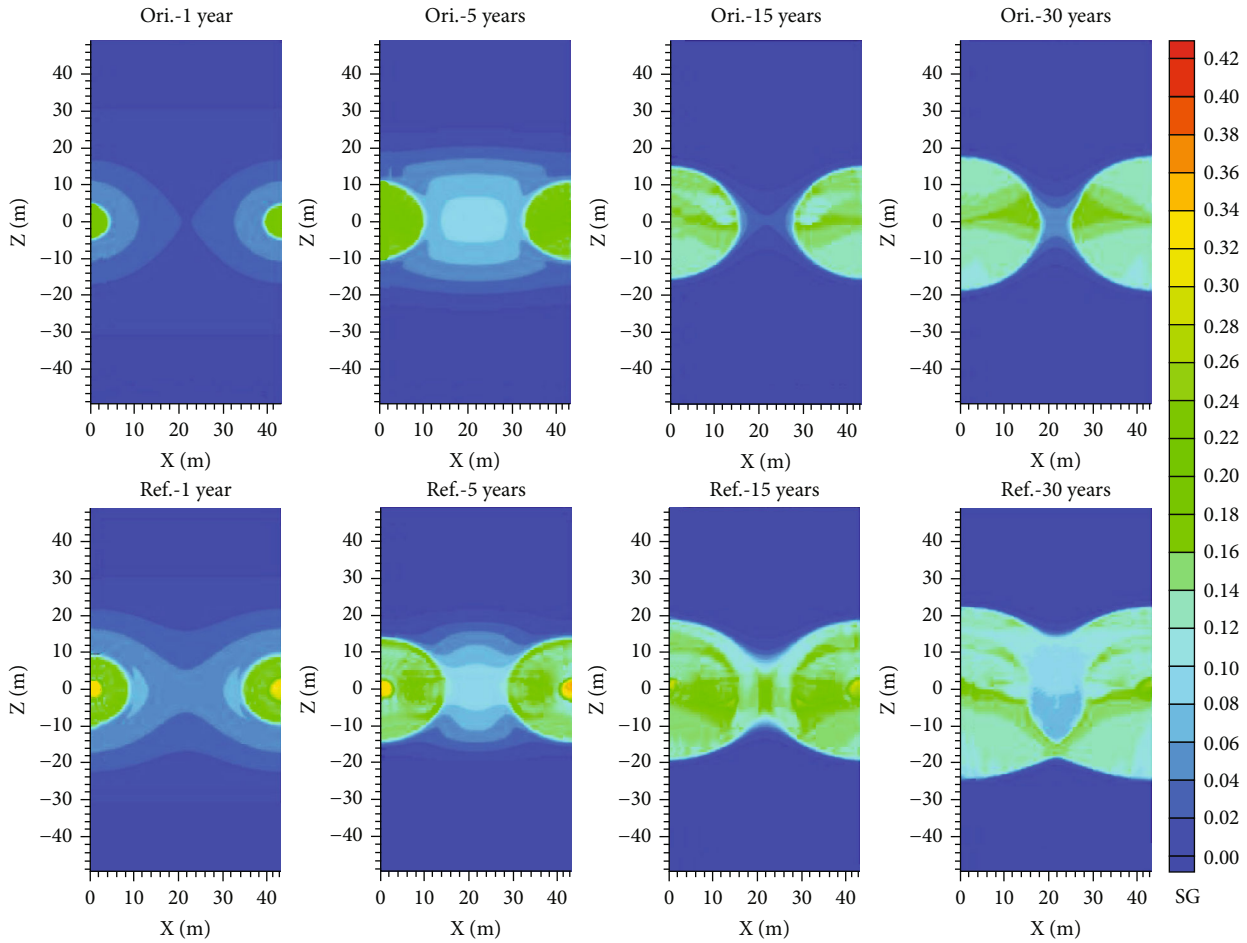

Figure 9: The spatial distributions of S_G in the original and reference cases.

Besides, the maximum value of R_{GW} in the original case is close to 94, but the maximum value of R_{GW} in the reference case exceeds 143; especially when $r_F = 5.0$ m, the maximum value of R_{GW} exceeds 173, which has achieved a huge breakthrough in the technical bottleneck for hydrate production in low-permeability reservoirs. In the case of $r_F = 5.0$ m, R_{GW} is lower than the reference case after about 6300 days of gas release from the hydrate deposits, which because of the remaining amount of hydrate deposits is less than 31%. With the decrease of hydrate resources, similar situations will occur under different r_F. That is to say, when the hydrate content in the simulation area decreases, R_{GW} in the production process will gradually decrease. This also shows that the use of fracturing technology can rapidly improve the decomposition rate of hydrate and greatly shorten the time of hydrate reservoir exploitation.

As shown in Figure 4, the final remaining hydrate deposits in the reference case are close to 28%, which indicates about 72% of the gas hydrate deposits have been decomposed compared to the only 41% in the original case. When $r_F = 5.0$ m, only about 17% of the hydrate in the simulated area will be left at the end of 30 years of exploitation, which has an important reference value for the layout of exploitation well spacing during the actual field exploitation of hydrates. Taking the 30-year production period as an example, the spacing of the double horizontal wells used in this project is 45 m. The hydrate between L_W and R_W can be basically recovered after the completion of mining when $r_F = 5.0$ m. Considering that the permeability in the fracturing area of the reference case is 100 mD, the permeability of the rocks around the hydraulic fracturing wells will lead to higher permeability, so it is recommended that the mining spacing of the dual horizontal wells in the permafrost area be 45~60 m.

3.2. Evaluation of the Productions with Different k_F

3.2.1. Gas and Water Production with Different k_F. Figures 5 and 6 show V_P and M_W from L_W and R_W at $r_F = 2.5$ m with $k_F = 1$, 2, 10, 100, and 1000 mD, respectively. As shown in Figure 5, at the end of the production period, it is found that the greater the k_F in the fracturing area, the maximum final V_P will be obtained. It is also found that even when k_F is 2 mD, the final V_P will also have a significant increase. This shows that it is a practical and effective technology to improve the permeability of the reservoir around the production well. By comparing the two groups of $k_F = 10$ mD and $k_F = 100$ mD, it is found that the gas production with

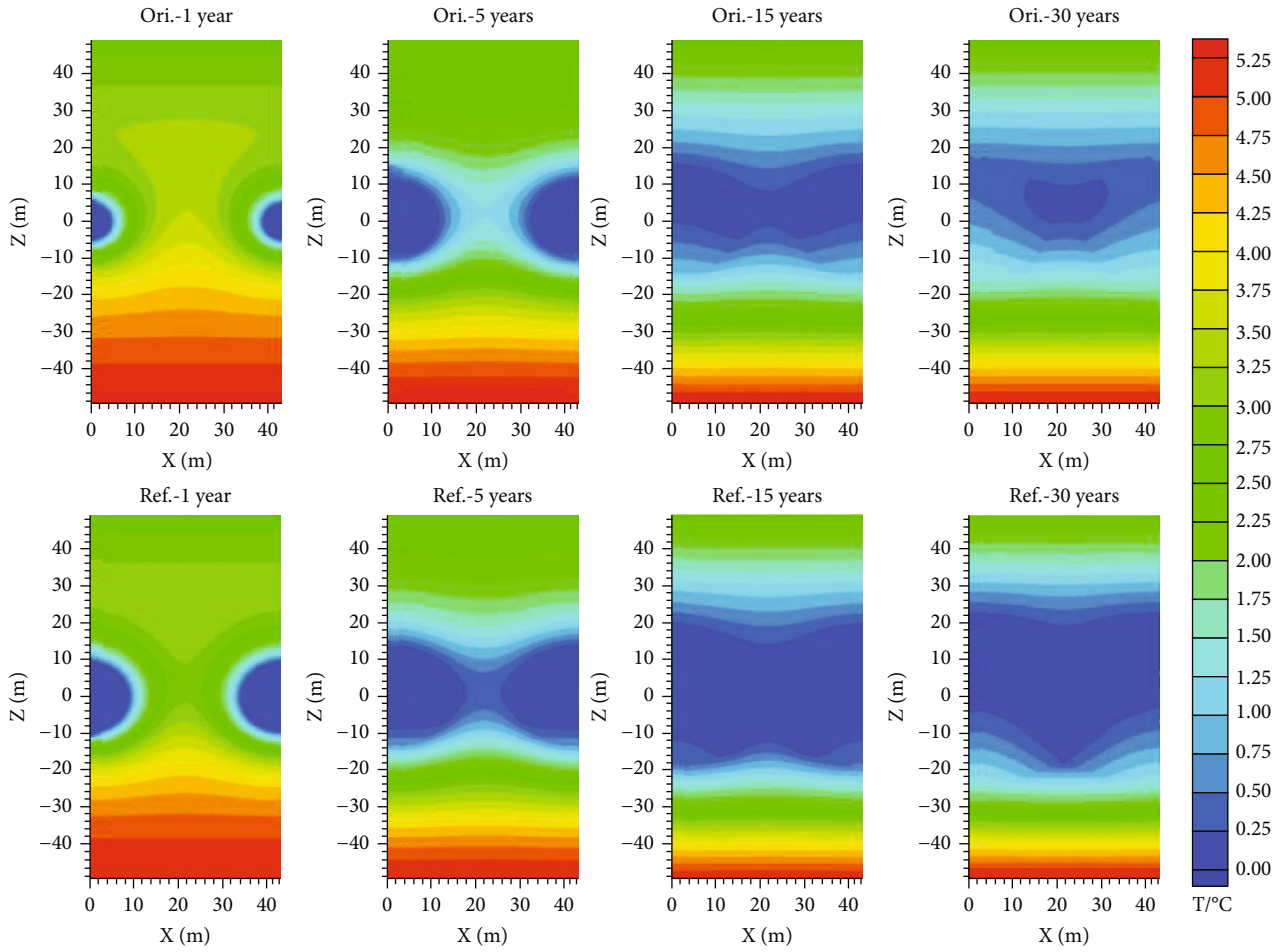

Figure 10: The spatial distributions of T in the original and reference cases.

$k_F = 100$ mD in the fracturing area is always higher than that with $k_F = 10$ mD; especially in the first 5000 days, it has obvious production effect. However, after 5000 days, the gas production rate of the group with $k_F = 10$ mD is slightly higher than that of the group with $k_F = 100$ mD, resulting in a close total gas production V_P at the end of production. When $k_F = 1000$ mD, it can be seen that the gas production increases rapidly and remains at the highest level all the time, and the gas production rate gradually decreases in the later period of production, mainly due to the small residual amount of hydrate reservoir between the two production wells. Therefore, if it is necessary to obtain the best gas production in a short time, the greater the k_F in the fracturing area, the better. If long-term production is required, k_F in the fracturing area can be reduced appropriately, but k_F in the fracturing area is recommended to be above 100 mD.

It can be seen from Figure 6 that the cumulative M_W increases with the increase of k_F. Compared with the original case and the case with $k_F = 1000$ mD, it is found that the cumulative M_W has increased from 5.67×10^5 kg to 9.89×10^5 kg, which is 1.74 times the original case. However, the gas production is from 2.2×10^4 m^3 to 4.0×10^4 m^3, which is 1.82 times the original case. The increase rate of V_P is still higher than that of M_W. This is basically consistent with the V_P and M_W characteristics in the expanded fracturing area. It shows that the increase of reservoir permeability around the production well is really conducive to gas production.

3.2.2. Gas-to-Water Ratio and the Remaining Hydrate Deposits with Different k_F. Figure 7 shows R_{GW} and R_H with $k_F = 1$, 2, 10, 100, and 1000 mD, respectively. In the initial one year, R_{GW} decreases sharply; afterwards, the decrease of R_{GW} slows down during the production period. The maximum value of R_{GW} in the case of $k_F = 1000$ mD is close to the reference case, which indicates there is an ideal value of k_F between 100 and 1000 mD. The increase in R_{GW} mainly concentrates on the previous decade and tends to stabilize after ten years, which is similar to the case described for the evaluation of the productions with different widths of the fracturing area mentioned above. The amount of resources directly affects the value of R_{GW}; in other words, the value of R_{GW} will decrease when R_H becomes little. In addition, it can be seen from the change curves of $g\,R_{GW}$ and R_H that when k_F in the fracturing area is between 1 and 10 mD, the change trend of the curves is relatively fluctuating. This may be due to the rapid depressurization propagation of the production well at the initial stage of production, which leads to the formation of solid ice in free

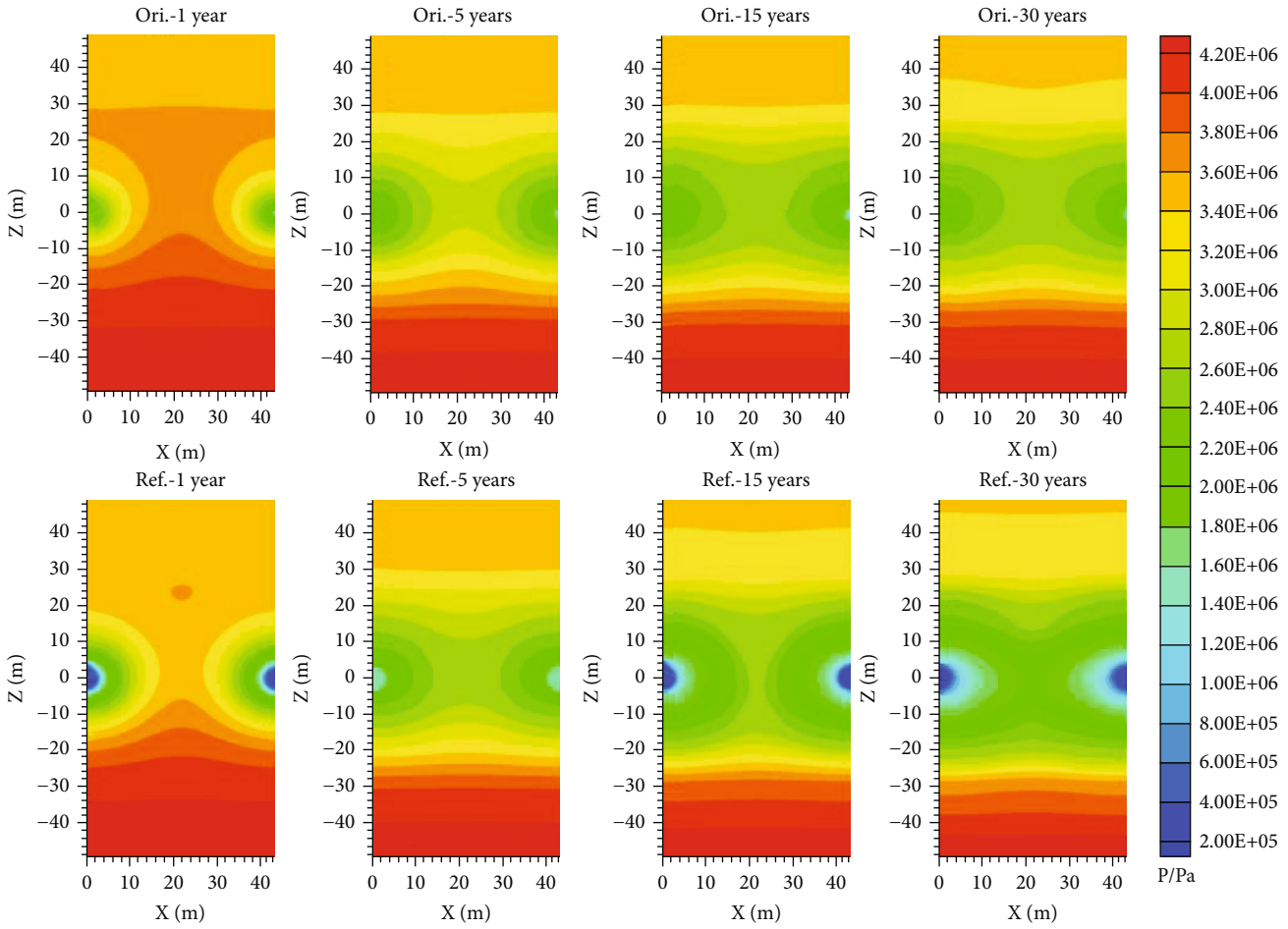

Figure 11: The spatial distributions of P in the original and reference cases.

water. The curves become smoother in the later stage of exploitation. This is because the reservoir around the production well no longer contains solid ice particles or ice particles no longer block most of the space where gas and liquid flow to the production well.

3.3. Spatial Distributions

3.3.1. Spatial Distributions of S_H. Figure 8 shows the spatial distribution of hydrate saturation (S_H) of the original case and the reference case at the mining time of 1, 5, 15, and 30 years, respectively. Only half L_W and R_W are considered to reveal the spatial distributions of pressure, temperature, hydrate, and gas saturations between two production wells during the decomposition of hydrate deposits. As shown in Figure 8, the hydrate layer decomposed is about 10 m in the first year, which is a great improvement for hydrate reservoirs with low permeability. The decomposition rate of hydrates on the X axis is slightly higher than that on the Z axis, due to the effect of pressure intermingling between the two production wells. In about 15 years, the hydrate deposits between the two production wells along the x axis finally connect with each other. After that, the dissociation of hydrate deposits is gradually toward the direction of OB and UB. Only a part of the hydrate deposits remain after constant pressure mining for 30 years. It was a meaningful phenomenon worth noting that the hydrate-dissociated areas were symmetrically distributed in the domain along the middle of the two production wells. In addition, the actual effect of the pure depressurization method for 30 years was not as good as that of fracturing combined with depressurization for 15 years. The comparison of the hydraulic fracturing combined with depressurization method in the reference case and pure depressurization method in the original case simulation results of spatial distributions of S_H at the time points $t = 1$, 15, and 30 years indicated the advantages of the hydraulic fracturing method.

In addition, it is found that when there is no hydrate on the connecting line between the two production wells, the breakthrough will occur and accelerate the decomposition of hydrate. When the hydrate gradually decomposes to the OB and UB boundary of HBL, it is found that the difficulty of hydrate decomposition increases, which may be caused by the formation of secondary hydrate. And S_H close to the UB is less than that of the OB, because the temperature at the bottom of the UB is higher than that of the OB, which makes the hydrate close to the UB easier to decompose. However, it is undeniable that the hydrate decomposition

near the OB and UB boundary of HBL is difficult, and it may need to improve the production well layout to achieve the production effect.

3.3.2. Spatial Distributions of S_G. Figure 9 shows the spatial distribution of gas saturation (S_G) of the original case and the reference case at the mining time of 1, 5, 15, and 30 years, respectively. The distribution of gas saturation reflected the decomposition of the hydrate deposits. The free gas released from the deposits is mainly concentrated in fracturing areas where gas and water flow faster with higher intrinsic permeability. The gas-accumulated areas are almost symmetrically distributed in the x axis at the value of $x =$ 22.5 m. In the first 15 years, S_G between the two wells gradually increases; after that, S_G decreases to a lower level. In the original case, the gas released between two production wells could not effectively flow into the production wells. At the end of the production period, there is still a large amount of free gas near the production wells. Compared to the gas saturation distributions in the hydrate sediments with higher intrinsic permeability of fracturing areas, the gas distribution within the original sediments is very limited. It is because the undissociated hydrate deposits as a permeability barrier to prevent the movement of gas and fluids. The free gas saturation is limited in the OB and UB due to the low effective permeability in both reference case and original case. The spatial distribution of S_G results showed that the effect of the use of hydraulic fracturing combined with depressurization method was very obvious.

3.3.3. Spatial Distributions of T. Figure 10 shows the spatial distribution of temperature (T) of the original case and the reference case at the mining time of 1, 5, 15, and 30 years, respectively. The temperatures in the HBL were mainly affected by the heat convection caused by the gas and fluid flow. The gas hydrate dissociation under depressurization was mainly promoted by the limited sensible heat of deposits near the production wells, and the temperature decreased to a lower level until the new temperature met the equilibrium condition. The two dissociation areas around the production wells connected with each other after 5 years, but the gas hydrate dissociated between the production wells connecting with each other at approximately 15 years, which indicated that there was a buffer period of pressure reduction before hydrate decomposition. The temperature at the bottom of the sediment was higher than that in the upper part because of the geothermal gradients. The temperature in the OB and UB was approximately constant, which indicated that there was little fluid flow into the HBL. Temperatures in most parts of the HBL had a large drop at the end of the 30-year production period, which indicated that most of the hydrate has been decomposed.

3.3.4. Spatial Distributions of P. Figure 11 shows the spatial distribution of pressure (P) of the original case and the reference case at the mining time of 1, 5, 15, and 30 years, respectively. The largest pressure drops appeared around both production wells and correspond to the hydrate dissociation region. Besides, a pressure gradient emerged between the two production wells because of the depressurization effect. The pressure gradient spread as time advances due to the free gas and fluid flowing into both production wells. Consequently, the pressure gradient areas were almost symmetrically distributed in the x axis at the value of $x = 22.5$ m. The pressure fluctuation tended to be stable around the production wells during the production period, which indicates a relatively stable hydrate dissociation and gas production process. In addition, the pressure distributions in the OB and UB were almost constant until the secondary hydrate disappeared to a very low level, which indicated that the OB and UB were sufficient to prevent the free gas and fluid from flowing to the hydrate HBL at the end of the simulation.

4. Conclusions

Based on the simulation results, the following conclusions could be drawn:

(1) The gas production rate and cumulative volume of gas for using hydraulic fracturing are both higher than that for using the pure depressurization method at the end of the simulation. The total cumulative methane gas in the reference case was almost 1.7 times that in the original case at the end of the 30-year production period

(2) In the reference case, more than 60% of gas production is produced in the first 10 years, and the final remaining hydrate deposits in the reference case are close to 28%, which indicates about 72% of the gas hydrate deposits have been decomposed compared to only 41% in the original case

(3) The maximum value of R_{GW} in the original case is close to 94, but the maximum value of R_{GW} in the reference case exceeds 143; especially when $r_F = 5.0$ m, the maximum value of R_{GW} exceeds 173, which has achieved a huge breakthrough in the technical bottleneck for hydrate production in low-permeability reservoirs

(4) The value of R_{GW} in the case of $k_F = 1000$ mD was close to that of the reference case, which indicates there is an ideal value of k_F between 100 and 1000 mD. The thickness of OB and UB is sufficient to prevent the free gas and fluid from flowing to the hydrate HBL at the end of the simulation

(5) The sensitivity analysis between the fracturing radius and the spacing between two horizontal wells optimizes the well layout and gas production parameters for hydrate production in permafrost regions

Data Availability

Data are available upon request.

Conflicts of Interest

The authors declare that they have no known competing financial interests or personal relationships that could have appeared to influence the work reported in this paper.

Authors' Contributions

All the authors contributed to publishing this paper. The main research idea was contributed by Li Chen, Dandan Liu, and Pengfei Shen; Pengfei Shen and Dandan Liu wrote the paper; Mao Xiyu was very helpful in reservoir structure modeling and grid division in the article; Chaoqun Cui provided verification on the feasibility of hydrate mining in this paper; Meng Li and Xinwang Li directed the writing of the article. All authors revised and approved the publication of the paper.

Acknowledgments

This work was financially supported by the Open Fund (PLN2022-21) of State Key Laboratory of Oil and Gas Reservoir Geology and Exploitation (Southwest Petroleum University), supported by the Science and Technology Project of Department of Education of Hebei Province (Grant No. QN2022027), supported by the Natural Science Foundation of Hebei Province (Grant Nos. E2020402075, E2022402014, and E2021402050), and supported by the Guangdong Provincial Key Laboratory of New and Renewable Energy Research and Development (Grant No. E239kf0601).

References

[1] Z. R. Chong, S. H. B. Yang, P. Babu, P. Linga, and X. S. Li, "Review of natural gas hydrates as an energy resource: prospects and challenges," *Applied Energy*, vol. 162, pp. 1633–1652, 2016.

[2] R. Boswell and T. S. Collett, "Current perspectives on gas hydrate resources," *Energy & Environmental Science*, vol. 4, no. 4, pp. 1206–1215, 2011.

[3] Y. F. Makogon, "Natural gas hydrates - a promising source of energy," *Journal of Natural Gas Science and Engineering*, vol. 2, no. 1, pp. 49–59, 2010.

[4] G. J. Moridis, T. S. Collett, M. Pooladi-Darvish et al., "Challenges, uncertainties, and issues facing gas production from gas-hydrate deposits," *SPE Reservoir Evaluation and Engineering*, vol. 14, no. 1, pp. 76–112, 2011.

[5] P. F. Shen, G. Li, J. F. Liu, Li, and Zhang, "Gas permeability and production potential of marine hydrate deposits in South China Sea," *Energies*, vol. 12, no. 21, p. 4117, 2019.

[6] B. Li, L. L. Chen, Q. C. Wan, X. Han, Y. Q. Wu, and Y. J. Luo, "Experimental study of frozen gas hydrate decomposition towards gas recovery from permafrost hydrate deposits below freezing point," *Fuel*, vol. 280, p. 118557, 2020.

[7] G. Li, B. Li, X. S. Li, Y. Zhang, and Y. Wang, "Experimental and numerical studies on gas production from methane hydrate in porous media by depressurization in pilot-scale hydrate simulator," *Energy & Fuels*, vol. 26, no. 10, pp. 6300–6310, 2012.

[8] G. Li, X. S. Li, Y. Wang, and Y. Zhang, "Production behavior of methane hydrate in porous media using huff and puff method in a novel three-dimensional simulator," *Energy*, vol. 36, no. 5, pp. 3170–3178, 2011.

[9] S. X. Li, Z. Q. Wang, X. H. Xu, R. Zheng, and J. Hou, "Experimental study on dissociation of hydrate reservoirs with different saturations by hot brine injection," *Journal of Natural Gas Science and Engineering*, vol. 46, pp. 555–562, 2017.

[10] E. A. Bondarev, I. I. Rozhin, V. V. Popov, and K. K. Argunova, "Underground storage of natural gas in hydrate state: primary injection stage," *Journal of Engineering Thermophysics*, vol. 27, no. 2, pp. 221–231, 2018.

[11] I. K. Gimaltdinov, M. V. Stolpovskii, and M. K. Khasanov, "Recovery of methane from gas hydrates in a porous medium by injection of carbon dioxide," *Journal of Applied Mechanics and Technical Physics*, vol. 59, no. 1, pp. 1–8, 2018.

[12] K. A. Birkedal, L. P. Hauge, A. Graue, and G. Ersland, "Transport mechanisms for CO_2-CH_4 exchange and safe CO_2 storage in hydrate-bearing sandstone," *Energies*, vol. 8, no. 5, pp. 4073–4095, 2015.

[13] P. F. Shen, G. Li, B. Li, and X. Li, "Coupling effect of porosity and hydrate saturation on the permeability of methane hydrate-bearing sediments," *Fuel*, vol. 269, p. 117425, 2020.

[14] Y. Wang, Z. Y. Song, T. Q. Mao, and C. Zhu, "Macro-meso fracture and instability behaviors of hollow-cylinder granite containing fissures subjected to freeze–thaw–fatigue loads," *Rock Mechanics and Rock Engineering*, vol. 55, no. 7, pp. 4051–4071, 2022.

[15] J. F. Li, J. L. Ye, X. W. Qin et al., "The first offshore natural gas hydrate production test in South China Sea," *China Geology*, vol. 1, no. 1, pp. 5–16, 2018.

[16] J. L. Ye, X. W. Qin, W. W. Xie et al., "The second natural gas hydrate production test in the South China Sea," *China Geology*, vol. 2, pp. 197–209, 2020.

[17] Y. Wang, Y. Su, Y. Xia, H. Wang, and X. Yi, "On the effect of confining pressure on fatigue failure of block-in-matrix soils exposed to multistage cyclic triaxial loads," *Fatigue & Fracture of Engineering Materials & Structures*, vol. 45, no. 9, pp. 2481–2498, 2022.

[18] Y. F. Makogon and R. Y. Omelchenko, "Commercial gas production from Messoyakha deposit in hydrate conditions," *Journal of Natural Gas Science and Engineering*, vol. 11, pp. 1–6, 2013.

[19] P. Babu, P. Linga, R. Kumar, and P. Englezos, "A review of the hydrate based gas separation (HBGS) process for carbon dioxide pre-combustion capture," *Energy*, vol. 85, pp. 261–279, 2015.

[20] R. Boswell, K. Rose, T. S. Collett et al., "Geologic controls on gas hydrate occurrence in the Mount Elbert prospect, Alaska North Slope," *Marine and Petroleum Geology*, vol. 28, no. 2, pp. 589–607, 2011.

[21] T. Mestdagh, J. Poort, and M. De Batist, "The sensitivity of gas hydrate reservoirs to climate change: perspectives from a new combined model for permafrost-related and marine settings," *Earth Science Reviews*, vol. 169, pp. 104–131, 2017.

[22] H. J. Jin and Q. Ma, "Impacts of permafrost degradation on carbon stocks and emissions under a warming climate: a review," *Atmosphere-Basel*, vol. 12, 2021.

[23] Y. Wang, J. Q. Han, Y. J. Xia, and D. Long, "New insights into the fracture evolution and instability warning predication for fissure-contained hollow-cylinder granite with different hole diameter under multi-stage cyclic loads," *Theoretical and Applied Fracture Mechanics*, vol. 119, article 103363, 2022.

[24] Y. M. Zhu, H. Wang, C. Chen, and T. Luo, "Effects of sand contents on mechanical characteristics of methane hydrate-bearing sediments in the permafrost," *Journal of Natural Gas Science and Engineering*, vol. 75, article 103129, 2020.

[25] T. Wang, "Gas hydrate resource potential and its exploration and development prospect of the Muli coalfield in the northeast Tibetan plateau," *Energy Exploration & Exploitation*, vol. 28, no. 3, pp. 147–157, 2010.

[26] Q. B. Wu, G. L. Jiang, and P. Zhang, "Assessing the permafrost temperature and thickness conditions favorable for the occurrence of gas hydrate in the Qinghai-Tibet Plateau," *Energy Conversion and Management*, vol. 51, no. 4, pp. 783–787, 2010.

[27] Y. H. Zhu, Y. Q. Zhang, H. J. Wen, Z. Q. Lu, and P. K. Wang, "Gas hydrates in the Qilian Mountain permafrost and their basic characteristics," *Acta Geos Sin-Ch*, vol. 31, no. 1, pp. 7–16, 2010.

[28] Z. Q. Lu, G. Y. Zhai, Y. H. Zhu et al., "New discovery of the permafrost gas hydrate accumulation in Qilian Mountain China," *China Geology*, vol. 2, pp. 306-307, 2018.

[29] Z. Q. Lu, S. Q. Tang, X. L. Luo et al., "A natural gas hydrate-oil-gas system in the Qilian Mountain permafrost area, northeast of Qinghai-Tibet Plateau," *China Geology*, vol. 3, no. 4, pp. 511–523, 2020.

[30] P. Wu, Y. H. Li, X. Sun, W. Liu, and Y. Song, "Mechanical characteristics of hydrate-bearing sediment: a review," *Energy & Fuels*, vol. 35, no. 2, pp. 1041–1057, 2021.

[31] P. F. Shen, Z. G. Sun, Y. J. Luo, X. Li, and C. Xiao, "Improving gas production of hydrate deposits by increasing reservoir permeability nearby production well in the South China Sea," *Energy Reports*, vol. 8, pp. 4416–4429, 2022.

[32] P. F. Shen, G. Li, X. S. Li, B. Li, and J. M. Zhang, "Application of fracturing technology to increase gas production in low-permeability hydrate reservoir: a numerical study," *Chinese Journal of Chemical Engineering*, vol. 34, pp. 267–277, 2021.

[33] Z. Lu, Y. Zhu, Y. Zhang, H. Wen, Y. Li, and C. Liu, "Gas hydrate occurrences in the Qilian Mountain permafrost, Qinghai Province, China," *Cold Regions Science and Technology*, vol. 66, no. 2–3, pp. 93–104, 2011.

[34] Y. Zhu, Y. Zhang, H. Wen et al., "Gas hydrates in the Qilian Mountain Permafrost, Qinghai, Northwest China," *Acta Geologica Sinica - English Edition*, vol. 84, no. 1, pp. 1–10, 2010.

[35] L. Qu, C. C. Zou, Z. Q. Lu et al., "Elastic-wave velocity characterization of gas hydrate-bearing fractured reservoirs in a permafrost area of the Qilian Mountain, Northwest China," *Marine and Petroleum Geology*, vol. 88, pp. 1047–1058, 2017.

[36] B. Li, Y. H. Sun, W. Guo et al., "The mechanism and verification analysis of permafrost-associated gas hydrate formation in the Qilian Mountain, Northwest China," *Marine and Petroleum Geology*, vol. 86, pp. 787–797, 2017.

[37] Z. Z. Lin, H. P. Pan, H. Fang, W. Gao, and D. Liu, "High-altitude well log evaluation of a permafrost gas hydrate reservoir in the Muli area of Qinghai, China," *Scientific Reports*, vol. 8, no. 1, p. 8, 2018.

[38] T. Yu, G. Q. Guan, D. Y. Wang, Y. Song, and A. Abudula, "Gas production enhancement from a multilayered hydrate reservoir in the South China Sea by hydraulic fracturing," *Energy & Fuels*, vol. 35, no. 15, pp. 12104–12118, 2021.

[39] X. Wang, Y. Sun, B. Li et al., "Reservoir stimulation of marine natural gas hydrate-a review," *Energy*, vol. 263, article 126120, 2023.

[40] L. U. Zhen-Quan, N. Sultan, C.-S. Jin et al., "Modeling on gas hydrate formation conditions in the Qinghai-Tibet plateau permafrost," *Chinese Journal of Geophysics*, vol. 52, pp. 157–168, 2009.